

# Ab Initio MR-CISD Study of Gas-Phase Basicity of Formamide in the First Excited Singlet State

Ivana Antol,<sup>†</sup> Mirjana Eckert-Maksic,<sup>\*,†</sup> and Hans Lischka<sup>\*,‡</sup>

Division of Organic Chemistry and Biochemistry, Rudjer Boškovic Institute, P.O.B. 108, HR-10002 Zagreb, Croatia and Institute for Theoretical Chemistry and Structural Biology, University of Vienna, Währingerstrasse 17, A-1090 Austria

Received: May 4, 2004; In Final Form: August 26, 2004

MR-CISD and MR-CISD+Q calculations have been carried out to investigate geometries, energies, and electronic absorption spectra of formamide and its O- and N-protonated forms. The vertical excitation energies for formamide are in good agreement with available experimental data and with the results of best calculations reported so far. Analysis of the calculated electronic absorption spectra reveals that the lowest excited state in the parent molecule and in its N-protonated form corresponds to the  $n-\pi^*$  valence excited state, whereas the O-protonated form shows the  $\pi-\pi^*$  excited valence state as the lowest one. The second excited valence states in the neutral molecule and the N-protonated ion are the  $\pi-\pi^*$  state, whereas it is the  $n-\pi^*$  state for the O-protonated formamide. Adiabatic excitation energies are reported for the first excited valence state of all three species with structures optimized at the MR-CISD level. All structures exhibit strong deviation from planarity characterized by pyramidalization of the C and the N atoms and rotation of the  $\text{NH}_2$  with respect to the plane of the COH group. It appears that oxygen is the most basic site of formamide both in the ground state and in the first singlet excited state. Its calculated gas-phase basicity (GB) and proton affinity (PA) in the latter are smaller than in the ground state by 2.1 kcal mol<sup>-1</sup> and 2.4 kcal mol<sup>-1</sup>, respectively. The difference in basicity between oxygen and nitrogen positions drops from 16 kcal mol<sup>-1</sup> (ground state) to 6 kcal mol<sup>-1</sup> (first singlet excited state). These results are analyzed within the Förster thermodynamic cycle.

## Introduction

Proton transfer is a fundamental process in chemical and biological systems. The excited state intramolecular proton transfer (ESIPT) occurs in a large variety of cases and has been investigated very thoroughly by various spectroscopic methods (see, e.g., refs 1–3). The understanding of proton-transfer processes in excited states is of great importance, for example, for fluorescence measurements of biomolecules,<sup>4</sup> for laser dyes<sup>5</sup> and photostabilizers,<sup>6</sup> for selecting matrixes in matrix-assisted laser desorption ionization (MALDI) mass spectrometry,<sup>7</sup> etc. In a recent study, we reported the results of multireference configuration interaction with singles and doubles (MR-CISD) and with inclusion of quadruple correction (MR-CISD+Q) calculations on protonated formaldehyde<sup>8</sup> in order to investigate the impact of protonation on the electronic structure of formaldehyde in its lowest vertically excited valence and Rydberg states. It was shown that protonation caused the Rydberg states to be shifted to higher energies by several eV. Moreover, the  $\pi-\pi^*$  valence state was energetically the second lowest state, about 1.50 eV below the first Rydberg  $n-3s$  state. This finding is in strong contrast to the case of formaldehyde where the  $\pi-\pi^*$  state is embedded within a series of Rydberg states (see, e.g., refs 9–12). The present study extends these investigations to the excited states of formamide and its O- and N-protonated forms. The electronic spectrum of formamide<sup>13–17</sup> and the protonation process of formamide in the ground

state<sup>18–26</sup> have been the subject of many experimental and theoretical studies in the past. This interest is not surprising, considering that this molecule is a prototype of a peptide linkage, the moiety that holds amino acid units in polypeptides and proteins together. Geometry relaxation effects for the excited states of formamide have been investigated by Li et al.<sup>27</sup> using the configuration interaction with singles (CIS) method. Rydberg states had not been taken into account in this work. To our knowledge, no theoretical calculations have been performed on protonated formamide in excited states.

For the study of the effect of electron excitations on proton affinities, the Förster thermodynamic cycle<sup>28,29</sup> in conjunction with absorption and/or fluorescence data is frequently used. Within this approach the change in basicity can be evaluated from a shift in the excitation energies between the protonated and neutral forms of a molecule in question. It is the purpose of this work to use formamide as the already mentioned model for a peptide bond and to study protonation processes in excited states and to assess the importance of different contributions (electronic and geometry relaxation effects) to the Förster cycle. For this purpose, we perform systematic high-level quantum chemical investigations not only on vertical excitation processes, but also explore the excited-state energy surfaces with the aim to locate and characterize energy minima. These investigations should provide a theoretical basis for future experimental protonation and proton-transfer studies of formamide and related molecules in the excited state.

## Theoretical Methods

In the first step, state averaged multiconfiguration self-consistent field (SA-MCSCF) calculations with equal weights

\* Corresponding authors. E-mails: mmaksic@emma.irb.hr; hans.lischka@univie.ac.at.

<sup>†</sup> Rudjer Boškovic Institute.

<sup>‡</sup> University of Vienna.

for six  $^1A'$  and five  $^1A''$  singlet states were performed in order to determine the molecular orbitals (MOs). The same number of states for state averaging and the same construction scheme for the active orbital space in the MCSCF and CI calculations has been used for formamide and its protonated forms. Similar to previous calculations on formaldehyde<sup>12</sup> and protonated formaldehyde<sup>8</sup> a valence complete active space (CAS) containing the  $8a'-12a'$  and  $1a''-3a''$  orbitals and 10 electrons was used in the MCSCF calculations for the description of the valence states. A detailed description of orbitals is given in the Discussion (section Orbital analysis). Additional auxiliary (AUX) orbitals  $13a'-15a'$  ( $3s$ ,  $3p_{\sigma}$ , and  $3p_{\sigma'}$ ) and  $4a''$  ( $3p_{\pi}$ ) were chosen for the description of Rydberg states. Only single excitations were allowed from the CAS into AUX orbitals. Three different reference spaces (small, intermediate, and large) were used in the MR-CISD calculations. The small reference space (MR-CISD(*s*)) comprised four orbitals ( $10a'$ ,  $1a''$ ,  $2a''$ , and  $3a''$ ) and six electrons. A pair of  $a'$  orbitals ( $9a'$  and  $11a'$ ) and two electrons were added to the intermediate reference space (MR-CISD(*i*)). In the large reference space employed in MR-CISD(*l*) calculations, the CAS was identical to the one used at the MCSCF level. The common characteristic of all three reference spaces is the restriction of CAS-AUX single excitations from the  $10a'$  ( $n$ ) and  $2a''$  ( $\pi$ ) orbitals of the CAS as compared to the full set of CAS orbitals in the MCSCF calculation. The final expansion space in terms of configuration state functions (CSFs) for the MR-CISD method is constructed by allowing all single and double excitations from all reference configurations into all virtual orbitals. Furthermore, the interacting space restriction was applied always,<sup>30</sup> and the three core orbitals have been kept frozen in all MR-CISD calculations. Additionally, size-extensivity corrections were computed by means of the extended Davidson method (MR-CISD+Q).<sup>31,32</sup> For the vertical excitations, the ground-state geometries optimized in  $C_s$  symmetry at the Møller–Plesset perturbation level to second order<sup>33–35</sup> (MP2)/cc-pVTZ<sup>36</sup> level were used. The basis set denoted d'-aug-cc-pVDZ was constructed from the aug-cc-pVDZ basis<sup>36,37</sup> by adding diffuse doubly (d-) augmented s- and p-functions on carbon, nitrogen, and oxygen and by d-augmented s-functions on hydrogen.<sup>38,39</sup> This basis set offers sufficient flexibility for adequate description of the 3s and 3p Rydberg orbitals while essentially suppressing Rydberg orbitals of higher  $n$  and  $l$  quantum numbers.

In the search for energy minima on the first excited-state potential energy surface, Rydberg states and Rydberg orbitals were not taken into account. This restriction was introduced on the basis of the analysis of the vertical electronic spectra of the studied species, which revealed that the first excited state for all molecules investigated had valence character. Accordingly, in this series of calculations the aug-cc-pVDZ basis set was used for geometry optimizations and only valence-type orbitals were included into the active space. Additionally, the standard cc-pVTZ basis set augmented with s and p diffuse functions taken from aug-cc-pVTZ (denoted as aug'-cc-pVTZ) was used in single-point calculations. The electronic ground state and the lowest excited state were included in the state averaging procedure with equal weights. SA-CASSCF geometry optimizations were performed first. The active space used in these calculations included all important  $\sigma$ ,  $\pi$ , and  $n$  orbitals (seven orbitals in total) with natural orbital occupations between 1.98 and 0.03 and eight electrons, which allowed us to take into account the essential features relevant for the geometry rearrangements processes. In the next step, all structures were reoptimized at the MR-CISD level of theory based on the SA-

CASSCF MOs. Analysis of the CI wave function showed that it could be well represented by the use of a three orbital and four electron CAS, which was finally used for the MR-CISD geometry optimizations. Moreover, the CI wave function was always monitored in order to verify that no other CSFs except those belonging to the reference wave function had a weight of more than 1%. Additionally, ground-state geometries of formamide and the respective protonated forms were optimized also by using the same methodology for the sake of comparison.

The SA-MCSCF and MR-CISD calculations were performed using the COLUMBUS program system.<sup>40–42</sup> Full geometry optimizations at a given molecular symmetry were performed by means of the analytic gradient method for MR-CISD wave functions.<sup>43–45</sup> The geometry optimizations and saddle point calculations were performed in natural internal coordinates as defined by Fogarasi et al.<sup>46</sup> using the direct inversion of iteration space for geometry optimization (GDIIIS) method.<sup>47</sup> The atomic orbital (AO) integrals and AO gradient integrals were computed with program modules taken from DALTON.<sup>48</sup> Harmonic vibrational frequencies were calculated by means of numerical differentiation of analytic gradients to determine the nature of the stationary point encountered. Thermodynamic quantities were calculated using the standard ideal gas, rigid rotor, and harmonic oscillator approximation. MP2 calculations have been done using the Gaussian98 program package.<sup>49</sup>

## Results and Discussion

### Vertical Electronic Excitations. Ground-State Properties.

Before discussing vertical excitation energies, we shall briefly comment on geometrical features of formamide and its protonated forms in the ground state. This is of interest, since it has been shown that the question whether the neutral molecule is planar or not is sensitive to the computational method (e.g., SCF, MBPT(2), MBPT(4), CCSD, and CCSD(T)) and basis set (e.g., DZP, TZP, TZP2, and PVTZ).<sup>50</sup> However, as has been found also in ref 50, energy differences between optimized planar and eventual nonplanar structures are insignificant, demonstrating the flatness of the potential energy surface in this respect. On the basis of the most extended calculations, it is believed that the true minimum-energy structure of formamide is planar, in agreement with experimental measurements.<sup>51</sup> Deviations from planarity occurred at the CASSCF and MR-CISD levels as well. However, in view of the previous findings,<sup>50</sup> we chose the planar ground-state structure for formamide, as reference points for the following calculations on excited states. The O- and N-protonated forms were found to possess  $C_s$  symmetry as well.<sup>20,23</sup> In addition to the CASSCF and MR-CISD geometry optimization for the ground state, MP2/cc-pVTZ optimizations and frequency calculations were performed also. The MP2 ground-state structures and vibrational frequencies were actually chosen for the calculation on vertical excitations and for ground-state zero-point vibrational energies.

Calculated geometry parameters obtained at the CASSCF and MR-CISD levels for all ground-state structures discussed in this work are given in Figure 1. They agree very well with the MP2 results and with available experimental data.<sup>51</sup> Complete Cartesian geometries including MP2/cc-pVTZ geometries are available as Supporting Material (see the end of the text for more information). Energetic results are listed in Table 1. Two minima were found for the O-protonated form, a trans structure with  $\text{OH}_4$  trans to the CN bond, and a cis structure with  $\text{OH}_4$  in cis position. The trans structure is more stable than the cis structure by 3.2 kcal mol<sup>-1</sup> (MP2/cc-pVTZ). Only the more stable trans structure was considered in the following.

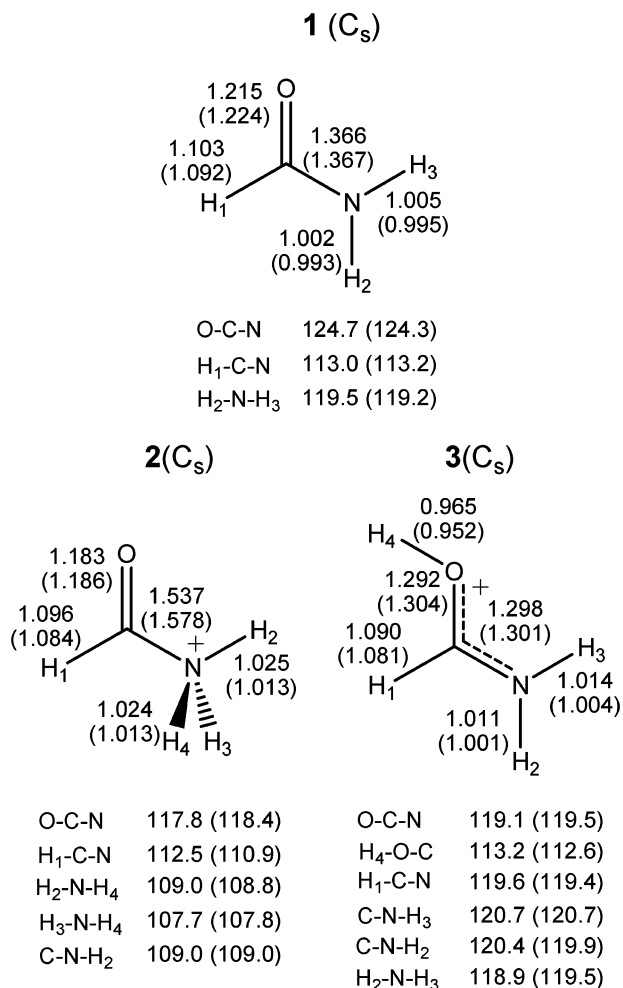


**Figure 1.** MR-CISD and CASSCF (in parentheses) optimized geometry parameters of planar structures **1–3** in the ground state. Bond lengths are in angstroms, and bond angles are in degrees.

**TABLE 1: Total Energies ( $E_{\text{tot}}$ /a.u.), Zero-Point Vibrational Energies (ZPVE/a.u.), and Relative Energies ( $E_{\text{rel}}$ /kcal mol<sup>-1</sup>) for Ground State Structures **1–3** Calculated at the MP2/cc-pVTZ, MR-CISD/aug-cc-pVDZ and MR-CISD+Q/aug-cc-pVDZ Levels of Theory**

	1	2	3
MP2/cc-pVTZ			
$E_{\text{tot}}$	-169.60545	-169.90910	-169.93563
ZPVE	0.04551	0.05864	0.06027
$E_{\text{rel}}^a$	207.2	16.6	0.0
MR-CISD/aug-cc-pVDZ			
$E_{\text{tot}}$	-169.43836	-169.74652	-169.77223
$E_{\text{rel}}^a$	209.5	16.1	0.0
MR-CISD+Q/aug-cc-pVDZ			
$E_{\text{tot}}$	-169.49204	-169.79789	-169.82402
$E_{\text{rel}}^a$	208.3	16.4	0.0

<sup>a</sup> Excluding ZPVE corrections.

The calculated energy difference between the O- and N-protonated formamide obtained at the MR-CISD+Q/aug-cc-pVDZ (16.4 kcal mol<sup>-1</sup>) and MP2/cc-pVTZ (16.6 kcal mol<sup>-1</sup>) levels is in good accord with the previously published value of 15.5 kcal mol<sup>-1</sup> calculated with the G2 method.<sup>20</sup> The MCSCF/aug-cc-pVDZ method reduces this energy gap to only 4.6 kcal mol<sup>-1</sup>. This clearly demonstrates the importance of inclusion of dynamical correlation energy in discussing relative energies of the protonated species.

**Orbital Analysis.** Since all ground-state structures have a symmetry plane, the active orbitals are separated into a' and a''

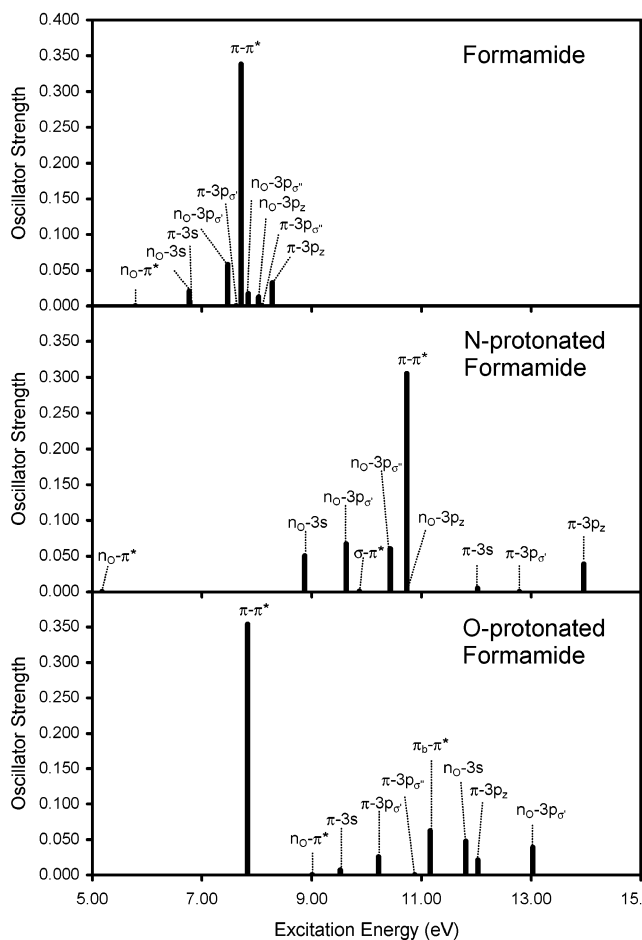


**Figure 2.** Comparison of the calculated electronic spectrum of formamide, N- and O-protonated formamide. MR-CISD+Q(*i*) excitation energies and MR-CISD(*i*) oscillator strengths are used.

subgroups. The group a' contains  $\sigma$ - and  $\sigma^*$ -type orbitals originating from combinations of the C–N and C–O bonds (with minor contributions from CH and NH bonds) and an in-plane nonbonding electron pair situated on the O-atom ( $n_{\text{O}}$ ). The  $\pi$ -system comprises three  $\pi$ -orbitals (1a'', 2a'' and 3a''), which will be denoted as  $\pi_{\text{b}}$ ,  $\pi$  and  $\pi^*$  hereafter. In formamide, the first one,  $\pi_{\text{b}}$ , is delocalized over the heavy-atom chain and is totally bonding, whereas the  $\pi$  orbital corresponds to the negative linear combination of the  $p_{\pi}$ -orbitals on the terminal atoms with the coefficients on the N atom being slightly larger than on the oxygen atom. In the N-protonated form, the  $\pi$  and  $\pi^*$  orbitals become more localized in the region of the C–O bond, whereas the  $\pi_{\text{b}}$  orbital transforms into a N-localized  $p_{\pi}$  orbital mixed with the antisymmetric combination of s orbitals located at the neighboring H atoms. In the O-protonated form, the shape of the  $\pi_{\text{b}}$ ,  $\pi$ , and  $\pi^*$  orbitals is quite similar to that in the neutral molecule. For the sake of simplicity, we shall use identical notation for these orbitals for all examined structures in the rest of discussion.

**Vertical Excitation Energies.** The calculated vertical excitation energies are summarized in Tables 2–4. Oscillator strengths (*f*) and the electronic radial spatial extents ( $\langle r^2 \rangle$ ), which are also displayed in these tables, are computed at the MR-CISD(*s*) and MR-CISD(*i*) levels of theory. All excitations are characterized by the symmetry of the excited state and by the predominant configuration describing this state. In addition, the results of MR-CISD+Q(*i*) calculations are shown graphically in Figure 2.

**TABLE 2: Vertical Excitation Energies (eV), Oscillator Strengths, and Expectation Values  $\langle r^2 \rangle$  (a.u.) for Singlet States of Formamide<sup>a</sup>**

state	MR-CISD									MR-CISD+Q			exp
	MCSF	small			intermediate			large	small	intermediate	large		
	$E_{exc}/eV$	$E_{exc}/eV$	f	$\langle r^2 \rangle$	$E_{exc}/eV$	f	$\langle r^2 \rangle$	$E_{exc}/eV$	$E_{exc}/eV$	$E_{exc}/eV$	$E_{exc}/eV$		
1A' (gr. state) <sup>b</sup>	-169.03346	-169.43411		38.3	-169.44415		38.4	-169.45653	-169.49506	-169.50285	-169.50773		
1A'' (n <sub>O</sub> -π*)	6.21	5.88	0.001	37.7	5.88	0.001	37.9	5.91	5.80	5.78	5.72	5.8	
2A'' (π-3s)	5.33	7.11	0.022	78.8	7.09	0.021	77.6	7.20	7.00	6.77	6.55	6.35	
2A' (n <sub>O</sub> -3s)	5.64	6.92	0.012	76.7	6.98	0.006	74.1	7.11	6.84	6.78	6.61		
3A' (n <sub>O</sub> -3p <sub>σ'</sub> )	6.23	7.49	0.056	88.5	7.61	0.058	87.8	7.76	7.48	7.47	7.32		
3A'' (π-3p <sub>σ'</sub> )	6.18	7.97	0.002	88.4	7.99	0.000	87.7	8.10	7.85	7.62	7.37		
4A' (π-π*)	9.24	8.30	0.225	79.3	8.25	0.338	59.0	8.24	7.92	7.71	7.60	7.36	
5A' (n <sub>O</sub> -3p <sub>σ''</sub> )	6.51	7.80	0.015	101.3	7.93	0.017	98.2	8.08	7.84	7.84	7.66	7.72	
4A'' (π-3p <sub>σ''</sub> )	6.6	8.52	0.000	100.5	8.54	0.001	101.8	8.65	8.34	8.03	7.82	8.02	
5A'' (n <sub>O</sub> -3p <sub>π</sub> )	6.59	7.91	0.012	101.7	8.06	0.013	100.0	8.23	8.01	8.08	7.90	7.83	
6A' (π-3p <sub>π</sub> )	6.57	8.69	0.198	62.9	8.64	0.033	88.7	8.71	8.15	8.28	8.06	8.22	

<sup>a</sup> MP2/cc-pVTZ geometries were used. Experimental values are taken from ref 13. <sup>b</sup> Total electronic energies (a.u.) are given for the ground state.

**TABLE 3: Vertical Excitation Energies (eV), Oscillator Strengths, and Expectation Values  $\langle r^2 \rangle$  (a.u.) for Singlet States of N-Protonated Formamide<sup>a</sup>**

state	MR-CISD									MR-CISD+Q		
	MCSF	small			intermediate			large	small	intermediate	large	
	$E_{exc}/eV$	$E_{exc}/eV$	f	$\langle r^2 \rangle$	$E_{exc}/eV$	f	$\langle r^2 \rangle$	$E_{exc}/eV$	$E_{exc}/eV$	$E_{exc}/eV$	$E_{exc}/eV$	
1A' (gr. state) <sup>b</sup>	-169.35794	-169.74191		26.5	-169.75321		26.6	-169.7647	-169.79913	-169.80695	-169.81094	
1A'' (n <sub>O</sub> -π*)	5.54	5.46	0.000	25.9	5.31	0.000	26.2	5.27	5.21	5.18	5.18	5.18
2A' (n <sub>O</sub> -3s)	8.60	9.08	0.023	43.2	9.15	0.050	41.6	9.24	8.92	8.87	8.72	
3A' (n <sub>O</sub> -3p <sub>σ'</sub> )	9.83	11.76	0.049	38.1	10.06	0.067	34.8	10.05	9.62	9.63	9.54	
2A'' (σ-π*)	11.45				11.32	0.001	26.5	10.31		9.87	9.68	
4A' (n <sub>O</sub> -3p <sub>σ''</sub> )	10.37	10.59	0.114	48.1	10.83	0.060	43.1	10.85	10.38	10.43	10.27	
3A'' (n <sub>O</sub> -3p <sub>π</sub> )	10.29	10.82	0.023	49.6	10.99	0.023	49.0	11.1	10.75	10.73	10.53	
5A' (π-π*)	11.57	11.32	0.292	34.6	11.34	0.305	38.6	11.26	10.77	10.73	10.67	
4A'' (π-3s)	11.62	12.08	0.004	44.3	12.12	0.005	43.0	12.27	12.15	12.02	11.91	
5A'' (π-3p <sub>σ'</sub> )	12.72	14.72	0.003	45.6	12.97	0.000	37.7		13.99	12.79		

<sup>a</sup> MP2/cc-pVTZ geometries were used. <sup>b</sup> Total electronic energies (a.u.) are given for the ground state.

**TABLE 4: Vertical Excitation Energies (eV), Oscillator Strengths, and Expectation Values  $\langle r^2 \rangle$  (a.u.) for Singlet States of O-Protonated Formamide<sup>a</sup>**

state	MR-CISD									MR-CISD+Q		
	MCSF	small			intermediate			large	small	intermediate	large	
	$E_{exc}/eV$	$E_{exc}/eV$	f	$\langle r^2 \rangle$	$E_{exc}/eV$	f	$\langle r^2 \rangle$	$E_{exc}/eV$	$E_{exc}/eV$	$E_{exc}/eV$	$E_{exc}/eV$	
1A' (gr. state) <sup>b</sup>	-169.36733	-169.76741		24.3	-169.77549		24.3	-169.78789	-169.82564	-169.83307	-169.83644	
2A' (π-π*)	8.67	8.27	0.387	24.6	8.19	0.354	24.7	8.14	7.89	7.83	7.78	
1A'' (n <sub>O</sub> -π*)	9.79	9.30	0.000	23.7	9.26	0.000	23.8	9.26	9.12	9.01	8.90	
2A'' (π-3s)	8.67	10.15	0.010	43.4	10.09	0.007	42.5	10.22	9.88	9.52	9.26	
3A'' (π-3p <sub>σ'</sub> )	9.55	10.95	0.022	44.8	10.89	0.025	44.5	10.94	10.57	10.22	10.00	
4A'' (π-3p <sub>σ''</sub> )	10.15	11.53	0.001	45.2	11.37	0.000	44.5	11.51	11.10	10.88	10.66	
3A' (π <sub>b</sub> -π*)	11.88	11.60	0.068	28.0	11.52	0.062	26.9	11.43	11.26	11.16	11.13	
4A' (n <sub>O</sub> -3s)	11.26	11.98	0.052	39.3	12.04	0.048	39.9	12.17	11.81	11.81	11.64	
5A' (π-3p <sub>π</sub> )	10.88	12.33	0.018	50.0	12.40	0.021	50.2	12.54	12.08	12.03	11.81	
6A' (n <sub>O</sub> -3p <sub>σ'</sub> )	12.72	13.71	0.038	45.2	13.75	0.039	45.0	13.78	13.11	13.03	12.73	

<sup>a</sup> MP2/cc-pVTZ geometries were used. <sup>b</sup> Total electronic energies (a.u.) are given for the ground state.

Perusal of the data presented in Table 2 illustrates that the general features of electronic excitations are already reproduced very well by the results obtained with the small reference space. Best agreement of excitation energies with available experi-

mental<sup>13</sup> and previously calculated<sup>14,15,16</sup> data for formamide is achieved with the MR-CISD+Q(*l*) method. MCSF results are given for reference purposes only. In the following, all excitation energies discussed refer to the calculation with the large



reference space if not specified otherwise. The lowest valence excited state of formamide, the  $n_O-\pi^*$  transition, is found at 5.72 eV, which is very close to the experimental value (5.8 eV). This state is followed by a pair of Rydberg  $n_O-3s$  and  $\pi-3s$  states at 6.55 and 6.61 eV, respectively. The oscillator strength of the  $n_O-3s$  state is significantly higher than for the  $\pi-3s$  state, which is in agreement with previously published results calculated by EOM-CC<sup>15</sup> and MR-CI<sup>13</sup> methods. The  $\pi-\pi^*$  valence state is computed at 7.60 eV, in quite good agreement with the experimental value (7.36 eV) and with the EOM-CCSD (7.66 eV<sup>15</sup>) and CASPT2 (7.41 eV<sup>16</sup>) results. From an analysis of the wave function, we find that the  $\pi-\pi^*$  state is quite heavily mixed with Rydberg character. This can be also seen from the large  $\langle r^2 \rangle$  value. The large oscillator strength is typical for a valence excitation. For a further detailed comparison of theoretical results with the experimental spectra, we refer especially to ref 15.

The calculated spectrum of N-protonated formamide resembles some of the features of the electronic spectrum of formamide, at least qualitatively (see Table 3 and Figure 2). For instance, the lowest excited state is the  $n_O-\pi^*$  state, which, however, has been moved by about 0.5 eV to lower excitation energy (5.18 eV) in comparison to the neutral molecule. Second, the  $\pi-\pi^*$  state falls into the region of Rydberg states and interacts strongly with them. The calculated spatial extent of this state (38.7 au, MR-CISD(*i*)) confirms this strong interaction. Contrary to the shift of the  $n_O-\pi^*$  state, the  $\pi-\pi^*$  state has a considerably larger excitation energy (10.67 eV) than in the neutral molecule (7.36 eV). Due to protonation on the N atom, the  $\pi$  system is essentially reduced to the CO bond, explaining the large destabilization. The Rydberg states are also shifted by several eV to higher excitation energies. This is particularly pronounced for the  $\pi$ -Rydberg states. In addition, a new  $\sigma-\pi^*$  valence state appeared with an excitation energy of 9.68 eV.

The calculated electronic absorption spectrum for O-protonated formamide differs considerably from that of the parent formamide molecule (see Table 4 and Figure 2). It is dominated by an intense transition to the  $\pi-\pi^*$  state, which is the lowest peak in the spectrum located at 7.78 eV. It is followed by the valence  $n_O-\pi^*$  state (8.90 eV). The  $\pi-\pi^*$  excitation remains almost unchanged as compared to that in the neutral molecule, whereas the shift of the  $n_O-\pi^*$  state is quite pronounced (3.18 eV). Such a strong increase in excitation energy of the  $n_O-\pi^*$  state can be rationalized by a strong interaction of the  $n_O$  orbital with the incoming proton. Since the proton approaches the O-atom in the symmetry plane, perturbation of the orthogonal  $\pi$  system is smaller resulting in a larger energetic separation of the  $n_O$  and  $\pi$  orbitals than in formamide. It is also interesting to note that the Rydberg transitions originating from the  $n_O$  and  $\pi$  orbitals are separated by more than 2 eV, whereas in formamide, these states appear in closely spaced pairs. The series of  $\pi$ -Rydberg states starts at 9.26 eV and is shifted by more than 2.5 eV to higher excitation energies as compared to formamide. Finally, a new  $\pi-\pi^*$  state (denoted as  $\pi_b-\pi^*$  in the Table 4) appears with an excitation energy of 11.13 eV.

To rationalize the large shift of the Rydberg states upon protonation, we use the Rydberg formula

$$E_{\text{exc}} = IP - RZ^2/(n - \delta)^2 \quad (1)$$

for fitting the energies of the Rydberg states.<sup>52</sup> IP is the ionization energy,  $R$  is the Rydberg constant,  $Z$  is the charge of the molecular core,  $n$  is the principal quantum number of the Rydberg orbital, and  $\delta$  is the quantum defect of the state of interest. In case of the protonated forms,  $Z = 2$ . The same active

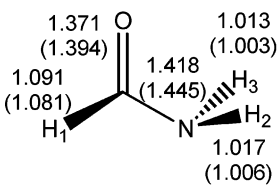
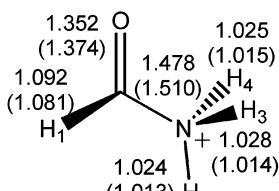
**TABLE 5: Vertical Ionization Potentials (eV) of Formamide and Its Protonated Forms and Quantum Defects Calculated at the MR-CISD+Q(*i*) Level of Theory by Using the d'-aug-cc-pVDZ Basis Set**

	formamide	N-protonated formamide	O-protonated formamide
$IP_v(n_O \rightarrow \infty)$ ( $1^2A' \leftarrow 1^1A'$ )	10.12	18.00	20.46
$\delta(n, 3s)$	0.982	0.558	0.492
$\delta(n, 3p_\sigma)$	0.734	0.450	0.294
$\delta(n, 3p_{\sigma'})$	0.557	0.318	
$\delta(n, 3p_\pi)$	0.449	0.263	
$IP_v(\pi \rightarrow \infty)$ ( $1^2A'' \leftarrow 1^1A'$ )	10.38	21.58	18.31
$\delta(\pi, 3s)$	1.058	1.807	1.756
$\delta(\pi, 3p_\sigma)$	0.778	1.756	1.703
$\delta(\pi, 3p_{\sigma'})$	0.566	1.664	1.647
$\delta(\pi, 3p_\pi)$	0.452		1.529

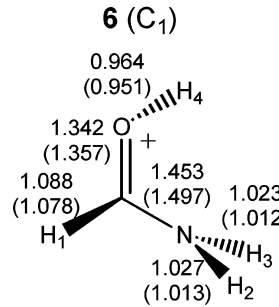
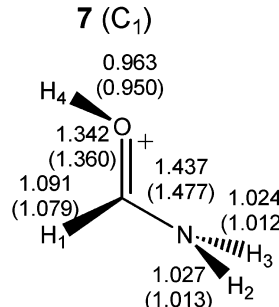
space (with one electron less) and the same geometry as for the MR-CISD(*i*) calculations of vertical excitations energies was used for the computation of the  ${}^2A'$  ( $n_O \rightarrow \infty$ ) and  ${}^2A''$  ( $\pi \rightarrow \infty$ ) ionized states of all three species. The computed ionization energies and quantum defects are summarized in Table 5. From the results, it is seen that the ionization energies of the protonated forms are substantially higher than for formamide itself. This fact is one of the main reasons for the large upward shift of the Rydberg states upon protonation. Additionally, the quantum defects are smaller for the  $n_O$ -Rydberg states as compared to formamide leading to a further relative increase of the excitation energies. Similar observations have been made for protonated formaldehyde.<sup>8</sup>

We shall conclude this section by comparing vertical excitation energies calculated with various reference spaces within the MR-CISD formalism. It is observed that exclusion of  $\sigma$  orbitals leads to a shift of most states to higher energies. Furthermore, excitations from the  $\pi$  orbital appear to be more affected than excitations from the  $n_O$  orbital. It should be also noted that the small reference space suppresses the  $\sigma-\pi^*$  state in the N-protonated form. However, it should be emphasized that reduction of reference space does not affect the energy of the lowest excited state. Generally, the lowest valence state (irrespective of its nature) is adequately described by the *small* reference space in all examined cases.

**Adiabatic Electronic Excitations.** In the first step, searches for minimum-energy structures of formamide were performed under restriction to  $C_s$  symmetry at the SA-CASSCF level starting from the ground-state geometries. State-averaging has been performed including the two lowest states. The vibrational analysis of the resulting structures showed that there were out-of-plane vibrational modes with imaginary frequencies and that, therefore, the assumption of  $C_s$  symmetry was not justified in the minimization procedure. Reoptimization of the excited-state structure of formamide by following the out-of-plane displacements in the direction of the imaginary frequency gave rise to the minimum energy structure **4** (Figure 3.). The same strategy has been applied for optimization of the N- and O-protonated forms resulting in structures **5–7** (Figure 3). All of the stationary structures **4–7** have been identified as energy minima without any imaginary frequencies at the SA-CASSCF level. In the next step, the MR-CISD method based on SA-MOs and the small reference space has been applied. The refined MR-CISD geometrical parameters are also shown in Figure 3. Complete Cartesian geometries are available as Supporting Information (see the end of the text for more information). Total electronic energies and adiabatic excitation energies for structures **4–7** calculated at CASSCF, MR-CISD, and MR-CISD+Q levels of theory have been collected in Table 6.

4 ( $C_1$ )		5 ( $C_1$ )	
			
O-C-N	112.6 (113.6)	O-C-N	109.0 (108.4)
H <sub>1</sub> -C-N	117.8 (117.3)	H <sub>1</sub> -C-N	115.6 (115.1)
C-N-H <sub>2</sub>	112.5 (111.5)	C-N-H <sub>2</sub>	109.9 (109.2)
C-N-H <sub>3</sub>	111.0 (113.2)	C-N-H <sub>3</sub>	112.4 (110.0)
H <sub>2</sub> -N-H <sub>3</sub>	108.4 (110.5)	C-N-H <sub>4</sub>	110.4 (111.8)
H <sub>3</sub> -N-C-O	-55.1 (-61.8)	H <sub>4</sub> -N-C-O	57.4 (56.5)
O-C-N-H <sub>2</sub>	66.6 (58.9)	O-C-N-H <sub>3</sub>	-61.3 (-64.2)
H <sub>2</sub> -N-C-H <sub>1</sub>	-69.4 (-76.2)	H <sub>3</sub> -N-C-H <sub>1</sub>	71.0 (68.8)
$\phi$	38.6 (52.2)	H <sub>1</sub> -C-N-H <sub>2</sub>	-49.9 (-51.9)
$\vartheta$	50.7 (38.8)	$\vartheta$	43.6 (38.8)
$\rho$	62.3 (69.0)		

6 ( $C_1$ )		7 ( $C_1$ )	
			
O-C-N	111.8 (112.3)	O-C-N	108.3 (107.9)
H <sub>1</sub> -C-N	114.1 (112.6)	H <sub>1</sub> -C-N	114.6 (114.5)
C-N-H <sub>2</sub>	121.3 (120.6)	C-N-H <sub>2</sub>	122.3 (121.4)
C-N-H <sub>3</sub>	121.9 (121.4)	C-N-H <sub>3</sub>	120.9 (120.3)
H <sub>2</sub> -N-H <sub>3</sub>	116.7 (117.9)	H <sub>2</sub> -N-H <sub>3</sub>	116.8 (118.2)
H <sub>4</sub> -O-C	113.5 (112.8)	H <sub>4</sub> -O-C	110.8 (110.4)
H <sub>3</sub> -N-C-O	-100.8 (-102.0)	H <sub>3</sub> -N-C-O	-100.9 (-98.9)
O-C-N-H <sub>2</sub>	74.6 (73.4)	O-C-N-H <sub>2</sub>	76.9 (77.2)
H <sub>2</sub> -N-C-H <sub>1</sub>	-60.7 (-59.4)	H <sub>2</sub> -N-C-H <sub>1</sub>	-64.0 (-62.7)
H <sub>4</sub> -O-C-N	71.3 (69.8)	H <sub>4</sub> -O-C-N	-174.9 (-164.2)
$\phi$	3.8 (3.8)	$\phi$	1.9 (3.2)
$\vartheta$	41.9 (44.0)	$\vartheta$	40.5 (41.5)
$\rho$	80.7 (80.7)	$\rho$	82.5 (80.8)

**Figure 3.** MR-CISD and CASSCF (in parentheses) optimized geometry parameters of structures 4–7 in the first excited state. Bond lengths are in angstroms, and bond angles are in degrees.

The geometrical relaxation of formamide resulted in pyramidalization of the carbon and nitrogen atoms as expected from qualitative considerations.<sup>27</sup> The pyramidal carbonyl group is a common feature of  $n_O-\pi^*$  excited carbonyl compounds. It results from an increase of electron density on carbon relative to the ground state (see Figure 4). Consequently, the stabilizing conjugative interaction between the carbonyl and the amine operative in the ground-state becomes repulsive, resulting in pyramidalization of the amino group. The extent of pyramidalization can be described by angles  $\phi$  and  $\vartheta$ , which are defined

**TABLE 6:** Calculated Total Energies ( $E_{\text{tot}}$ /a.u.), Zero-Point Vibrational Energies (ZPVE/a.u.), and Adiabatic Excitation Energies ( $E_{\text{exc}}$ /eV) for Structures 4–7<sup>a,b</sup>

	4	5	6	7
CASSCF				
$E_{\text{tot}}$	-168.88763	-169.21678	-169.20121	-169.20503
ZPVE	0.04498	0.06045	0.06095	0.06023
$E_{\text{exc}}$	5.00	4.01	5.04	4.94
MR-CISD				
$E_{\text{tot}}$	-169.27879 (-169.39452)	-169.60119 (169.71800)	-169.59819 (-169.71625)	-169.60284 (-169.72155)
$E_{\text{exc}}$	4.33 (4.48)	3.90 (4.09)	4.73 (4.89)	4.60 (4.74)
MR-CISD+Q				
$E_{\text{tot}}$	-169.33147 (-169.45744)	-169.65122 (-169.78125)	-169.65539 (-169.78353)	-169.66045 (-169.78862)
$E_{\text{exc}}$	4.36 (4.47)	3.94 (4.02)	4.58 (4.72)	4.44 (4.58)

<sup>a</sup> Adiabatic excitation energies for structures 4, 5, and 6–7 are calculated with respect to structures 1, 2, and 3, respectively. <sup>b</sup> Results in parentheses are calculated at the MR-CI+Q/aug'-cc-pVTZ level.

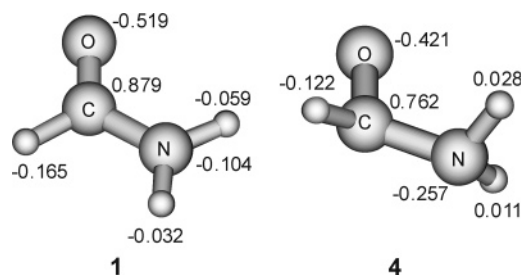


**Figure 4.** Comparison of net atomic Mulliken charges for formamide in 1 (ground state) and 4 (first excited state) as computed from MR-CISD/aug-cc-pVDZ calculations.

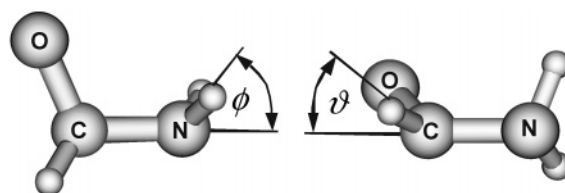


**Figure 5.** Definition of  $\phi$  and  $\vartheta$  angles.

as the smallest angles between the CN bond and the orthogonal projection of the C–N bond onto the NH<sub>2</sub> and CHO planes, respectively (Figure 5). In structure 4, they assume the values 38.6° and 50.7°, respectively. In addition, the NH<sub>2</sub> group is rotated with respect to the plane of the COH group by  $\rho = 62.3^\circ$ , presumably due to a tendency of the nitrogen lone pair to be directed away from the oxygen atom. The structure with opposite orientation of the NH<sub>2</sub> group is by 1.56 kcal mol<sup>-1</sup> higher in energy and has a negative imaginary frequency. Both, the C–O and C–N bond distances become stretched by 0.16 and 0.05 Å. Their weakening is also reflected in the shift of harmonic vibrational frequencies of the CO and CN stretching modes (computed at the SA-CASSCF/aug-cc-pVDZ level) from 1800.3 and 1325.2 cm<sup>-1</sup> in the ground state to 1061.4 and 1121.5 cm<sup>-1</sup> in the excited state, respectively. For comparison, the respective experimental ground-state frequencies are 1754.1 and 1258.2 cm<sup>-1</sup>.<sup>53</sup> The fact that the formamide geometry deviates from planarity compares well with previous calculations using the CIS/6-31G\* method.<sup>27</sup> However, we find a significantly stronger stretched CO bond (1.371 Å) as compared to the CIS results (1.272 Å).

Similar to the parent molecule, the first excited singlet state of N-protonated formamide is characterized by a strongly pyramidalized carbon atom. Furthermore, a shortening of the CO bond by 0.019 Å and stretching of the CN bond by 0.060 Å is observed with respect to excited-state formamide **4**. These trends, although less pronounced, are in accord with geometrical changes observed upon N-protonation in the ground state (−0.032 and 0.171 Å). The orientation of the NH<sub>3</sub> group with respect to the CO bond in the excited-state structure **5** is almost opposite to that in the ground-state structure **2**. The dihedral angle O–C–N–H<sub>2</sub> is 184.9° and 0.0° in excited and ground state, respectively.

It is important to note that, despite the strong deformation of the excited-state structures **4** and **5** with respect to the planar ground state, the character of the HOMO and LUMO orbitals involved in the excitation resembles qualitatively the valence n<sub>O</sub> and π\* orbitals described in the discussion of the vertical electronic spectrum. However, it should be noted that rotation of the NH<sub>2</sub> group in **4** causes a decrease of the conjugative interaction between the amino and carbonyl groups. Consequently, the π and π\* orbitals become more localized in the C–O bond and resemble corresponding formaldehyde orbitals, whereas the π<sub>b</sub> orbital becomes fully localized in the region of the amino group. In the N-protonated form **5**, localization of the π and π\* orbitals on CO is indicated by CN bond stretching.

For O-protonated formamide, two structures, **6** and **7**, were found, with the latter being more stable by 3.18 kcal mol<sup>−1</sup> (MR-CISD+Q). In this case, geometry optimization started in the planar structure of the π–π\* state. During the rotation of the NH<sub>2</sub> group the π orbital transformed into pure a n<sub>N</sub> orbital and the character of first excited state can be classified as n<sub>N</sub>–π\*. In both structures, pyramidalization of the N-atom is negligible (φ = 3.8° and 1.9° in **6** and **7**, respectively) and the NH<sub>2</sub> group is found to be almost perpendicular to the O–C–N plane. Furthermore, shortening of the CO bonds in **6** and **7** relative to the same bond in neutral formamide **4** is observed. On the other hand, the CN bond lengths are stretched relative to **4** (1.453 Å (**6**) and 1.437 Å (**7**) vs 1.418 Å (**4**)). The stretching of the CN bond in **6** or **7** of about 0.15 Å is even more remarkable when compared to the ground-state structure **3**. All of these changes are indicative of a diminution of the conjugative interaction between the CO and the NH<sub>2</sub> groups.

The adiabatic excitation energies of formamide and its N- (**5**) and O-protonated structures (**6**–**7**) calculated with respect to the ground state of formamide (**1**), N- (**2**) and the lowest energy O-protonated form **3**, are summarized in Table 6. As expected from the large geometry relaxation effects, all adiabatic excitation energies differ considerably from the vertical ones. The largest effect is noted for the O-protonated form ( $E_{\text{exc}}(\text{vert.}) = 7.89$  eV vs  $E_{\text{exc}}(\text{adiab.}) = 4.44$  eV). On the other hand, geometry relaxation in formamide and in N-protonated formamide has a smaller effect on the excitation energy and is of similar magnitude (1.3 and 1.4 eV, respectively), implying that the energy of the n<sub>O</sub>–π\* state is less influenced by geometry relaxation than the π–π\* state in O-protonated formamide. Single-point MR-CISD calculations using the MR-CISD/aug-cc-pVDZ geometries have been performed with the aug'-cc-pVTZ basis. The results given in Table 6 show changes of about 0.1 eV at the MR-CISD+Q level with respect to the aug-cc-pVDZ basis demonstrating that the latter basis is sufficiently flexible for our purposes.

**Gas-Phase Basicity of Formamide in the First Excited State.** The gas-phase basicity, GB, of a base B is formally defined as the standard Gibbs free energy change ( $\Delta G^\circ$ ) for

the reaction in eq 2, the corresponding proton affinity, PA, being the standard enthalpy change ( $\Delta H^\circ$ ) for the same reaction



Accordingly, the PA of formamide can be calculated from ab initio data following thermodynamic eq 3

$$\begin{aligned} \text{PA} &= \Delta H^\circ = H^\circ(\text{B}) - H^\circ(\text{BH}^+) + H^\circ(\text{H}^+) \\ &= E_{\text{tot}}(\text{B}) + \text{ZPVE}(\text{B}) + T_c(\text{B}) - E_{\text{tot}}(\text{BH}^+) - \\ &\quad \text{ZPVE}(\text{BH}^+) - T_c(\text{BH}^+) + (5/2)RT \quad (3) \end{aligned}$$

where B and BH<sup>+</sup> stands for the neutral and one of the protonated forms of formamide, respectively, and T<sub>c</sub> is the temperature correction to the internal energy.

To compute the GB

$$\begin{aligned} \text{GB} &= \Delta G^\circ = G^\circ(\text{B}) - G^\circ(\text{BH}^+) + G^\circ(\text{H}^+) \\ &= \Delta H^\circ - T\Delta S^\circ \quad (4) \end{aligned}$$

the reaction entropy

$$\Delta S^\circ = S^\circ(\text{B}) - S^\circ(\text{BH}^+) + S^\circ(\text{H}^+) \quad (5)$$

has to be evaluated. For the entropy of the proton S<sup>°</sup>(H<sup>+</sup>), the experimental value of 26.040 cal mol<sup>−1</sup> K<sup>−1</sup> was taken from ref 54. The S<sup>°</sup>(B) and S<sup>°</sup>(BH<sup>+</sup>) terms were evaluated as the sum of vibrational, rotational and translational contributions in the standard harmonic oscillator-rigid rotor ideal gas approximation. Total electronic energies E<sub>tot</sub> for the optimized structures were taken from MR-CISD+Q calculations. Zero-point vibrational energies (ZPVE) and temperature corrections (T<sub>c</sub>) at 298 K, as well as standard entropies were calculated from MP2 and CASSCF data in the ground and excited states, respectively. It is customary to scale the calculated harmonic frequencies in order to improve agreement with experiment.<sup>55</sup> Unfortunately, there is no recommended empirical factor for MCSCF calculations for excited states and, therefore, no scaling factors were used in this work.

The calculated values of standard reaction enthalpies, entropies and Gibbs free energies are collected in Table 7 along with the corresponding data for the ground state protonation. Before dealing with base property of formamide we shall briefly comment enthalpy and entropy contributions to the gas-phase basicity separately. In all examined cases, the entropy contribution of about 8 kcal mol<sup>−1</sup> is quite small relative to the total value of the GB. Moreover, it is practically constant for all cases listed in Table 7. Therefore, the proton affinity as well as the gas phase basicity can equally serve for evaluation of intrinsic base properties and basicity trends of formamide.

The gas-phase basicity and proton affinity of formamide have been determined experimentally<sup>56</sup> for the ground-state allowing us to test the accuracy of our calculations in this case. The corresponding calculated values, related to protonation at the O-site are 192.4 and 200.8 kcal mol<sup>−1</sup>, which is by 3.3 and 4.3 kcal mol<sup>−1</sup> higher than the experimental values (189.1 and 196.5 kcal mol<sup>−1</sup>, respectively).<sup>56</sup> Use of the aug'-cc-pVTZ basis slightly deteriorates the agreement.

Analysis of the results in Table 7 obtained with the aug-cc-pVDZ basis shows that the oxygen basicity in formamide decreases upon excitation to the first excited state. Calculated GB and PA values are 190.3 and 198.4 kcal mol<sup>−1</sup>, respectively. On the contrary, the N-atom becomes more basic by 7 kcal mol<sup>−1</sup> than in the ground state. Consequently, the strong



**TABLE 7: Standard Reaction Enthalpies, Entropies, and Gibbs Free Energies for Protonation of Formamide in Ground and First Excited State<sup>a,b</sup>**

	$H^\circ/\text{a.u.}$	$S^\circ/\text{cal K}^{-1}\text{mol}^{-1}$	$G^\circ/\text{a.u.}$	$\Delta H^\circ/\text{kcal mol}^{-1}$	$\Delta S^\circ/\text{cal mol}^{-1}\text{K}^{-1}$	$\Delta G^\circ/\text{kcal mol}^{-1}$
Ground State						
1	-169.43967 (-169.57162)	62.134	-169.46918 (-169.60113)			
2	-169.73262 (-169.86599)	63.533	-169.76279 (-169.89616)	185.31 (186.20)	25.60	177.67 (178.56)
3	-169.75738 (-169.89281)	60.691	-169.78620 (-169.92163)	200.84 (203.03)	28.44	192.36 (194.55)
Excited State						
4	-169.28175 (-169.40772)	62.185	-169.31128 (-169.43727)			
5	-169.58602 (-169.71605)	62.923	-169.61590 (-169.74595)	192.41 (194.96)	26.26	184.58 (187.13)
6	-169.58975 (-169.71789)	62.042	-169.61921 (-169.74737)	194.75 (196.11)	27.14	186.66 (188.02)
7	-169.59548 (-169.72365)	62.148	-169.62499 (-169.75318)	198.35 (199.73)	27.04	190.29 (191.67)

<sup>a</sup> Total energies taken from MR-CI+Q calculations; ZPVE,  $T_c$ , and  $S^\circ$  taken from MP2/aug-cc-pVDZ and CASSCF/aug-cc-pVDZ calculations for ground and excited states, respectively. <sup>b</sup> Results in parentheses are calculated with total energies taken from MR-CI+Q/aug-cc-pVTZ calculations.

preference for protonation at the O-atom in the ground state (15 kcal mol<sup>-1</sup>) diminishes to only 6 kcal mol<sup>-1</sup>. Very similar results are obtained with the aug'-cc-pVTZ basis.

The relative enhancement and reduction of N- and O-basicity compared to the ground state can be qualitatively rationalized by changes in the total electron densities on the N- and O-atoms induced by the electronic excitation of formamide, as demonstrated by a comparison of Mulliken charges for structures **1** and **4** (Figure 4). An alternative way of evaluating the effect of excitation on acid-base properties of molecules is offered by the Förster thermodynamic cycle.<sup>28,29</sup> This scheme was used here to evaluate electronic and geometry-relaxation contribution to basicity changes. The shift of vertical excitation energies corresponds to electronic effects, whereas geometry-relaxation is included in the adiabatic difference of excitation energies. The calculated difference between vertical excitation energies of formamide and O-protonated formamide is about 2.1 eV leading to a decrease of basicity by 48 kcal mol<sup>-1</sup>. Geometry relaxation cancels this change to a large extent (~ 46 kcal mol<sup>-1</sup>) so that the net effect is almost vanishing. On the other hand, the electronic effect contributes to a basicity enhancement in N-protonated form by 0.59 eV (~14 kcal mol<sup>-1</sup>) as judged from the vertical excitation energy differences. Geometry optimization, again, counteracts this change, but only by ca. 5 kcal mol<sup>-1</sup> this time.

## Conclusions

The MR-CISD and MR-CISD+Q methods have been applied to calculate vertical excitation energies and oscillator strengths of formamide and its N- and O-protonated forms. The vertical excitation energies for formamide are in good agreement with available experimental data and with the results of best calculations reported so far. Analysis of the calculated electronic absorption spectra shows that the lowest excited state in the parent molecule and its N-protonated form corresponds to the  $n_O-\pi^*$  valence excited state with a very weak transition intensity. The second valence excited state is the  $\pi-\pi^*$  state, which falls into the region of Rydberg states and was found to be strongly mixed with them. In contrast to that, in the O-protonated form the  $\pi-\pi^*$  valence excited state is the lowest one, whereas the  $n_O-\pi^*$  valence state appears as the second excited state. Full geometry optimizations for the lowest excited state of each compound have been performed. It was found that all minimum energy structures of formamide and its protonated

forms in the first excited state exhibited strong deviation from planarity characterized by pyramidalization of the carbon and the nitrogen atoms and rotation of the NH<sub>2</sub> with respect to the plane of CHO group.

Finally, the intrinsic basicity and proton affinity of O- and N-protonation sites in formamide in the first singlet excited state has been calculated. It is found that the O-atom is more basic than the N-atom by 6 kcal mol<sup>-1</sup>, which is 9 kcal mol<sup>-1</sup> less than in the ground state. This results from two opposing effects: (a) a decrease of oxygen basicity (by 2 kcal mol<sup>-1</sup>) and (b) an increase in basicity of nitrogen atom (by 7 kcal mol<sup>-1</sup>). As concerns the application of the Förster cycle to evaluate excited-state proton affinities we find that vertical excitations lead to large shifts with respect to the ground state. However, using optimized (equilibrium) data, these effects are largely counterbalanced by geometry relaxation effects.

**Acknowledgment.** The authors acknowledge support by the WTZ treaty between Austria and Croatia (Project Nos. 11/2002 and 9/2004) and by the Austrian Science fund within the framework of the Special Research Program F16 and project P14817-N03 (H.L.). The work in Zagreb (I.A., and M.E.M.) has been supported by the Ministry of Science and Technology of Croatia through project 0098056 and COSTD26 project, working group 01-03). The calculations were performed in part on the Schroedinger II Linux cluster of the Vienna University Computer Center.

**Supporting Information Available:** CASSCF and MR-CISD energies and Cartesian geometries for all structures and electronic states investigated in this work, MP2 results for the ground state. This material is available free of charge via the Internet at <http://pubs.acs.org>.

## References and Notes

- (1) Arnaut, L.; Formosinho, S. J. *J. Photochem. Photobiol. A: Chem.* **1993**, *75*, 1.
- (2) Ormson, S. M.; Brown, R. G. *Prog. React. Kinet.* **1994**, *19*, 45.
- (3) Douhal, A.; Lahmani, F.; Zewail, A. H. *Chem. Phys.* **1996**, *207*, 477.
- (4) (a) Das, R.; Mitra, S.; Nath, D.; Mukherjee, S. *J. Phys. Chem.* **1996**, *100*, 14514. (b) Sytnik A.; Kasha, M. *Proc. Natl. Acad. Sci. U.S.A.* **1994**, *91*, 8627.
- (5) Uzhinov, B. M.; Druzhinin, S. I. *Uspekhi Khimii.* **1998**, *67*, 140.



- (6) Werner, T.; Woessner, G.; Kramer, H. E. A. In *Photodegradation and Photostabilization of Coatings*; Pappas, S. P., Winslow, F. H., Eds.; American Chemical Society: Washington, DC, 1981; p 151.
- (7) Olumee, Z.; Vertes, A. *J. Phys. Chem. B* **1998**, *102*, 6118.
- (8) Antol, I.; Eckert-Maksić, M.; Müller, T.; Dallos, M.; Lischka, H. *Chem. Phys. Lett.* **2003**, *374*, 587.
- (9) (a) Hachey, M. R. J.; Bruna, P. J.; Grein, F. *J. Phys. Chem.* **1995**, *99*, 8050. (b) Bruna, P. J.; Hachey, M. R. J.; Grein, F. *J. Phys. Chem.* **1995**, *99*, 16576.
- (10) Merchán, M.; Roos, B. O. *Theor. Chim. Acta* **1995**, *92*, 227.
- (11) Gwaltney, S. R.; Bartlett, R. J. *Chem. Phys. Lett.* **1995**, *241*, 26.
- (12) Müller, T.; Lischka, H. *Theor. Chem. Acc.* **2001**, *106*, 369.
- (13) Gingell, J. M.; Mason, N. J.; Zhao, H.; Walker, I. C.; Siggel, M. R. F. *Chem. Phys.* **1997**, *220*, 191 and references therein.
- (14) Hirst, J. D.; Hirst, D. M.; Brooks, C. L., III. *J. Phys. Chem.* **1996**, *100*, 13487.
- (15) Szalay, P. G.; Fogarasi, G. *Chem. Phys. Lett.* **1997**, *270*, 406.
- (16) Serrano-Andrés, L.; Fülischer, P. *J. Am. Chem. Soc.* **1996**, *118*, 12190.
- (17) Chen, X.-B.; Fang, W.-H.; Fang, D.-C. *J. Am. Chem. Soc.* **2003**, *125*, 9689.
- (18) Lin, H.-Y.; Ridge, D. P.; Uggerud, E.; Vulpius, T. *J. Am. Chem. Soc.* **1994**, *116*, 2996.
- (19) Wu, C.-C.; Jiang, J. C.; Hahndorf, I.; Chaudhuri, C.; Lee, Y. T.; Chang, H.-C. *J. Phys. Chem. A* **2000**, *104*, 9556.
- (20) Tortajada, J.; Leon, E.; Morizur, J.-P.; Luna, A.; Mø, O.; Yáñez, M. *J. Phys. Chem.* **1995**, *99*, 13890.
- (21) Cho, S. J.; Cui, C.; Lee, J. Y.; Park, J. K.; Suh, B.; Park, J.; Kim, B. H.; Kim, K. S. *J. Org. Chem.* **1997**, *62*, 4068.
- (22) Ou, M.-C.; Chu, S.-Y. *J. Phys. Chem.* **1995**, *99*, 556.
- (23) Pranata, J.; Davis, G. D. *J. Phys. Chem.* **1995**, *99*, 14340.
- (24) Bagno, A.; Scorrano, G. *J. Phys. Chem.* **1996**, *100*, 1536.
- (25) Kamitakahara, A.; Pranata, J. *J. Mol. Struct. (THEOCHEM)* **1998**, *429*, 61.
- (26) Krug, J. P.; Popelier, P. L. A.; Bader, R. F. W. *J. Phys. Chem.* **1992**, *96*, 7604.
- (27) Li, Y.; Garrell, R. L.; Houk, K. N. *J. Am. Chem. Soc.* **1991**, *113*, 5895.
- (28) Förster, Th. *Z. Electrochem., Angew. Phys. Chem.* **1950**, *54*, 51.
- (29) Freiser, B. S.; Beauchamp, J. L. *J. Am. Chem. Soc.* **1977**, *99*, 3216.
- (30) Bunge, A. *J. Chem. Phys.* **1970**, *53*, 20.
- (31) Langhoff, S. R.; Davidson, E. R. *Int. J. Quantum. Chem.* **1974**, *8*, 61.
- (32) Bruna, P. J.; Peyerimhoff, S. D.; Buenker, R. J. *Chem. Phys. Lett.* **1981**, *72*, 278.
- (33) Head-Gordon, M.; Pople, J. A.; Frisch, M. J. *Chem. Phys. Lett.* **1988**, *153*, 503.
- (34) Frisch, M. J.; Head-Gordon, M.; Pople, J. A. *Chem. Phys. Lett.* **1990**, *166*, 275.
- (35) Frisch, M. J.; Head-Gordon, M.; Pople, J. A. *Chem. Phys. Lett.* **1990**, *166*, 281.
- (36) Dunning, T. H., Jr. *J. Chem. Phys.*, **1989**, *90*, 1007.
- (37) Kendall, R. A.; Dunning, T. H., Jr.; Harrison, R. J. *J. Chem. Phys.* **1992**, *96*, 6796.
- (38) Woon, D. E.; Dunning, T. H., Jr. *J. Chem. Phys.* **1994**, *100*, 2975.
- (39) von Mourik, T.; Wilson, A. K.; Dunning, T. H., Jr. *Mol. Phys.* **1992**, *96*, 6796.
- (40) Shepard, R.; Shavitt, I.; Pitzer, R. M.; Comeau, D. C.; Pepper, M.; Lischka, H.; Szalay, P. G.; Ahlrichs, R.; Brown, F. B.; Zhao, J. *Int. J. Quantum Chem.* **1988**, *S22*, 149.
- (41) Lischka, H.; Shepard, R.; Pitzer, R. M.; Shavitt, I.; Dallos, M.; Müller, Th.; Szalay, P. G.; Seth, M.; Kedziora, G. S.; Yabushita, S.; Zhang, Z. *Phys. Chem. Chem. Phys.* **2001**, *3*, 664.
- (42) COLUMBUS, An Ab Initio Electronic Structure Program, release 5.9 written by: Lischka, H.; Shepard, R.; Shavitt, I.; Pitzer, R. M.; Dallos, M.; Müller, Th.; Szalay, P. G.; Brown, F. B.; Ahlrichs, R.; Böhm, H. J.; Chang, A.; Comeau, D. C.; Gdanitz, R.; Dachsels, H.; Erhard, C.; Ernzerhof, M.; Höchtel, P.; Irle, S.; Kedziora, G.; Kovar, T.; Parasuk, V.; Pepper, M.; Scharf, P.; Schiffer, H.; Schindler, M.; Schüler, M.; Zhao, J.-G. 2003.
- (43) Shepard, R.; Lischka, H.; Szalay, P. G.; Kovar, T.; Ernzerhof, M. *J. J. Chem. Phys.* **1992**, *96*, 2085.
- (44) Shepard, R. In *Modern Electronic Structure Theory Part I*; Yarkony, D. R., Ed.; World Scientific: Singapore, 1995; p 345.
- (45) Lischka, H.; Dallos, M.; Shepard, R. *Mol. Phys.* **2002**, *100*, 1647.
- (46) Fogarasi, G.; Zhou, X.; Taylor, P. W.; Pulay, P. *J. Am. Chem. Soc.* **1992**, *114*, 8191.
- (47) Cszaszar P.; Pulay, P. *J. Mol. Struct.* **1984**, *114*, 31.
- (48) DALTON, an ab initio electronic structure program, Release 1.0, written by Helgaker, T.; Jensen, H. J. Aa.; Jørgensen, P.; Olsen, J.; Ruud, K.; Agren, H.; Andersen, T.; Bak, K. L.; Bakken, V.; Christiansen, O.; Dahle, P.; Dalskov, E. K.; Enevoldsen, T.; Heiberg, H.; Hettema, H.; Jonsson, D.; Kirpekar, S.; Kobayashi, R.; Koch, H.; Mikkelsen, K. V.; Norman, P.; Packer, M. J.; Saue, T.; Taylor, P. R.; Vahtras, O. 1997.
- (49) Frisch, M. J.; Trucks, G. W.; Schlegel, H. B.; Scuseria, G. E.; Robb, M. A.; Cheeseman, J. R.; Zakrzewski, V. G.; Montgomery, J. A., Jr.; Stratmann, R. E.; Burant, J. C.; Dapprich, S.; Millam, J. M.; Daniels, A. D.; Kudin, K. N.; Strain, M. C.; Farkas, O.; Tomasi, J.; Barone, V.; Cossi, M.; Cammi, R.; Mennucci, B.; Pomelli, C.; Adamo, C.; Clifford, S.; Ochterski, J.; Petersson, G. A.; Ayala, P. Y.; Cui, Q.; Morokuma, K.; Malick, D. K.; Rabuck, A. D.; Raghavachari, K.; Foresman, J. B.; Cioslowski, J.; Ortiz, J. V.; Baboul, A. G.; Stefanov, B. B.; Liu, G.; Liashenko, A.; Piskorz, P.; Komaromi, I.; Gomperts, R.; Martin, R. L.; Fox, D. J.; Keith, T.; Al-Laham, M. A.; Peng, C. Y.; Nanayakkara, A.; Gonzalez, C.; Challacombe, M.; Gill, P. M. W.; Johnson, B.; Chen, W.; Wong, M. W.; Andres, J. L.; Gonzalez, C.; Head-Gordon, M.; Replogle, E. S.; Pople, J. A. *Gaussian 98*, revision A.7; Gaussian, Inc.: Pittsburgh, PA, 1998.
- (50) Foragasi, G.; Szalay, P. G. *J. Phys. Chem. A* **1997**, *101*, 1400 and references therein.
- (51) Hirota, E.; Sugisaki, R.; Nielsen, C. J.; Sørensen, G. O. *J. Mol. Spectrosc.* **1974**, *49*, 251.
- (52) Sándorfy, C. In *The Role of Rydberg States in Spectroscopy and Photochemistry*; Sándorfy, C., Ed.; Kluwer Academic Publishers: Dordrecht, The Netherlands, 1999; Vol. 20, pp 1–20.
- (53) McNaughton, D.; Evans, C. J.; Lane, S.; Nielsen, C. J. *J. Mol. Spectrosc.* **1999**, *193*, 104.
- (54) Chase, M. W., Jr., *NIST-JANAF Thermochemical Tables, Fourth Edition*, *J. Phys. Chem. Ref. Data, Monograph 9*, **1998**, 1–1951.
- (55) Scott, A. P.; Radom, L. *J. Phys. Chem.* **1996**, *100*, 16502.
- (56) Hunter, E. P.; Lias, S. G. *J. Phys. Chem. Ref. Data* **1998**, *27*, 413.